Molecular Orientation in Helical and All-Trans Oligo(ethylene glycol)-Terminated Assemblies on Gold: Results of ab Initio Modeling

L. Malysheva,[†] A. Onipko,[‡] R. Valiokas,[#,§] and B. Liedberg*[,#]

Bogolyubov Institute for Theoretical Physics, Kiev, 03143, Ukraine, Division of Physics, Luleå University of Technology, S-971 87 Luleå, Sweden, and Division of Molecular Physics, Department of Physics, Chemistry and Biology, Linköping University, S-581 83 Linköping, Sweden

Received: May 9, 2005; In Final Form: June 30, 2005

The structural properties of self-assembled monolayers (SAMs) of oligo(ethylene glycol) (OEG)-terminated and amide-containing alkanethiols ($HS(CH_2)_{15}CONH(CH_2CH_2O)_6H$ and related molecules with shorter alkyl or OEG portions) on gold are addressed. Optimized geometry of the molecular constituents, characteristic vibration frequencies, and transition dipole moments are obtained using density-functional theory methods with gradient corrections. These data are used to simulate IR reflection−absorption (RA) spectra associated with different OEG conformations. It is shown that the positions and relative intensities of all characteristic peaks in the fingerprint region are accurately reproduced by the model spectra within a narrow range of the tilt and rotation angles of the alkyl plane, which turns out to be nearly the same for the helical and all-trans OEG conformations. In contrast, the tilt of the OEG axis changes considerably under conformational transition from helical to all-trans OEG. By means of ab initio modeling, we also clarify other details of the molecular structure and orientation, including lateral hydrogen bonding, the latter of which is readily possessed by the SAMs in focus. These results are crucial for understanding phase and folding characteristics of OEG SAMs and other complex molecular assemblies. They are also expected to contribute to an improved understanding of the interaction with water, ions, and ultimately biological macromolecules.

1. Introduction

In the current contribution, we utilize ab initio modeling to address a specific class of OEG SAMs on Au(111) supporting surfaces, which has been studied recently by means of standard and temperature-programmed IR reflection−absorption (RA) spectroscopy.[1,2] The SAMs, formed by self-assembly of $HS(CH_2)_mCONH-(CH_2CH_2O)_nH$ (the OEG portion $(CH_2CH_2O)_nH$ of these molecules is denoted below as EG_n), exhibit unique conformational properties depending on the nature of the supporting lattice, the OEG length, and the substrate temperature. The all-trans conformation was found experimentally in shorter OEG SAMs on gold[1,2] and on silver[3] whereas longer OEGs on gold[1,2] generally adopt the helical conformation. EG_6-terminated SAMs, however, were shown to undergo reversible temperature-driven conformational phase transitions near 60 °C from helical to all-trans.[1,2] The latter observation provides a valuable set of experimental data that is needed for adjusting the results of the ab initio modeling of the different helical and all-trans OEG conformations.

Ab initio methods have been used extensively in studies of substantially shorter and less complicated molecules than those encountered here.[4−7] We as well as others are using the density functional theory (DFT) method for obtaining reliable equilibrium molecular geometries, vibrational frequencies, and transition dipole moments (TDMs) for OEG molecules.[6,8,9] Combining the results from ab initio modeling of $HS(CH_2)_mCONH-EG_n$ with experimental RA spectra measured for a given conformation enables us to propose the optimized geometry of the molecule and its orientation (including mutual orientation of the alkyl, amide, and OEG portions) within the respective SAMs on gold. In general terms, such a modeling provides a deeper insight into the nature of the temperature-driven phase transitions observed in OEG SAMs. To elucidate the role of the length of the molecular segments and of the different OEG conformations, we model the vibrational spectra of molecules with different lengths of the alkyl portion ($m = 11$ and 15) and different lengths ($n = 4$ and 6) and conformations (all-trans and helical) of the OEG portion. The obtained results allow us also to address issues related to in-plane stabilization of the OEG assemblies through the formation of a lateral hydrogen bonding network between neighboring amide groups.[10] We discuss also future possibilities to include intermolecular as well as substrate interactions in the modeling.

2. Details of Calculations

The optimized geometry and TDMs of vibrational modes, which have been used here to model the IR RA spectra of specifically oriented $HS(CH_2)_mCONH-EG_n$ molecules, were calculated by using the DFT method with a BP86 exchange-correlation functional (with 6-31G* basis set) as provided by the Gaussian-03 suite of programs. Earlier we have shown that this method gives satisfactory reproducibility of RA spectra without frequency scaling in the fingerprint region.[8,9] Likewise in the cited works, the values of all the vibrational frequencies in the fingerprint region (900−1400 cm^{-1}) are given unscaled, while the frequencies of the amide II and amide III peaks are multiplied by 1.037 (see section 4).

* To whom correspondence should be addressed. E-mail: bolie@ifm.liu.se.

[†] Bogolyubov Institute for Theoretical Physics.

[‡] Luleå University of Technology.

[#] Linköping University.

[§] Present address: Molecular Compounds Physics Laboratory, Institute of Physics, Savanoriu 231, LT-02300 Vilnius, Lithuania.

10.1021/jp052395k CCC: $30.25
Published on Web 08/09/2005

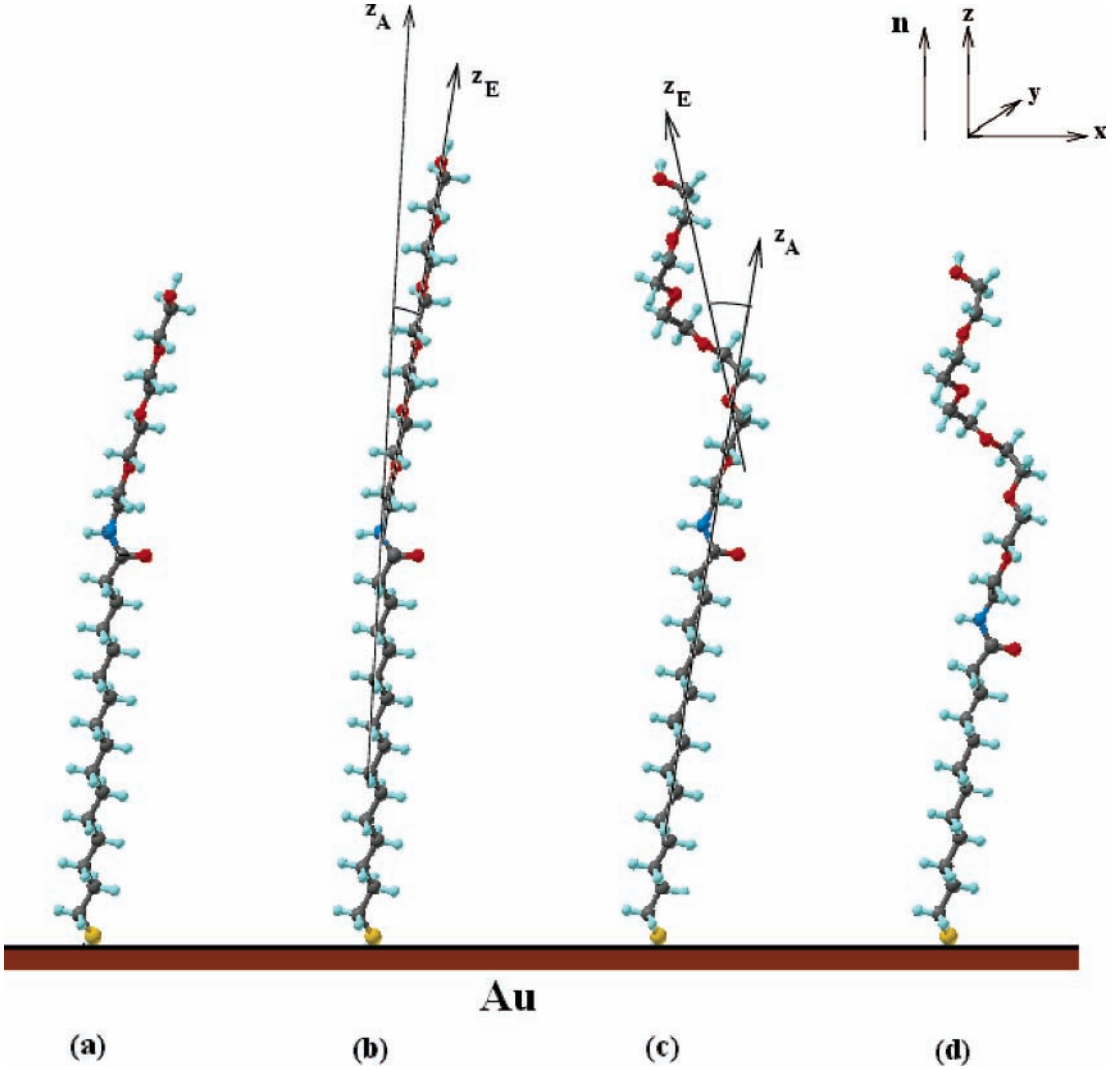

Figure 1. Representation of optimal orientations of molecules **1**−**3** with respect to the SAM substrate surface: (a) $HS(CH_2)_{15}CONH-EG_4$ (trans) **(1-t)** for $\theta_A = 26°$, $\psi_A = -62°$, $\varphi_A = -80°$; (b) $HS(CH_2)_{15}CONH-EG_6$ (trans) **(2-t)** for $\theta_A = 26°$, $\psi_A = -65°$, $\varphi_A = -82°$; (c) $HS(CH_2)_{15}CONH-EG_6$ (helix) **(2-h)** for $\theta_A = 26°$, $\psi_A = -62°$, $\varphi_A = -72°$; (d) $HS(CH_2)_{11}CONH-EG_6$ (helix) **(3-h)** for $\theta_A = 26°$, $\psi_A = -58°$, $\varphi_A = -74°$.

In focus are RA spectra of the following molecules: $HS(CH_2)_{15}CONH-EG_4$ with the EG_4 portion in the all-trans conformation (**1-t**), $HS(CH_2)_{15}CONH-EG_6$ with the EG_6 part in the all-trans (**2-t**) and helical (**2-h**) conformations, and $HS(CH_2)_{11}CONH-EG_6$ with the EG_6 portion in the helical conformation (**3-h**). Molecules **1**−**3** are represented in Figure 1. Experimental data for these compounds have been published in ref 2. Our modeling of the IR response is based on the assumption that the molecular vibrations are weakly perturbed by the molecule−substrate and intermolecular interactions. Moreover, the results of ab initio calculations of the mode intensities for a single molecule (which in the output are given in the so-called standard orientation chosen by Gaussian for maximum calculation efficiency), that is, the TDM $\mu^{(i)}$ of each normal mode, were projected onto Cartesian coordinate axes. These axes were chosen to be rigidly connected with the CCC plane as illustrated in Figure 2a. In terms of tilt and rotation angles of the alkyl chain, θ_A and ψ_A, respectively, the component of $\mu_\perp^{(i)}$, which is perpendicular to the supporting surface, is given by the following relation,

$$\mu_\perp^{(i)} = -\mu_x^{(i)} \sin\theta_A \cos\psi_A + \mu_y^{(i)} \sin\theta_A \sin\psi_A + \mu_z^{(i)} \cos\theta_A \quad (1)$$

whereas the squared TDM $(\mu_{av}^{(i)})^2$ for modeling the spectra of randomly oriented molecules can be written as

$$(\mu_{av}^{(i)})^2 = \frac{1}{3}[(\mu_x^{(i)})^2 + (\mu_y^{(i)})^2 + (\mu_z^{(i)})^2]. \quad (2)$$

The model spectra are obtained as the sum of Lorentzian-shaped peaks, each centered at the fundamental mode frequency ν_i, having the half width at half-maximum (hwhm) which is determined by parameter σ (in cm^{-1}). In such an approximation, the frequency dependence of the RA spectrum is given by,

$$I(\nu) = I_0 \frac{\sigma}{\pi} \sum_i \frac{(\mu^{(i)})^2}{(\nu - \nu_i)^2 + \sigma^2} \quad (3)$$

where $\mu^{(i)}$ equals $\mu_\perp^{(i)}$ for the molecules self-assembled on gold and $\mu_{av}^{(i)}$ for the randomly oriented molecules. The fitting parameter σ and a dimensional scaling factor I_0 are specified later on. RA spectra are calculated here in the frequency interval of 900−1700 cm^{-1} that includes the fingerprint and amide regions.

3. Geometry and Orientation of OEG-SAM Components

3.1. Optimized Geometry. Geometry optimization is the first step in computing vibrational spectra. For the observed proper-

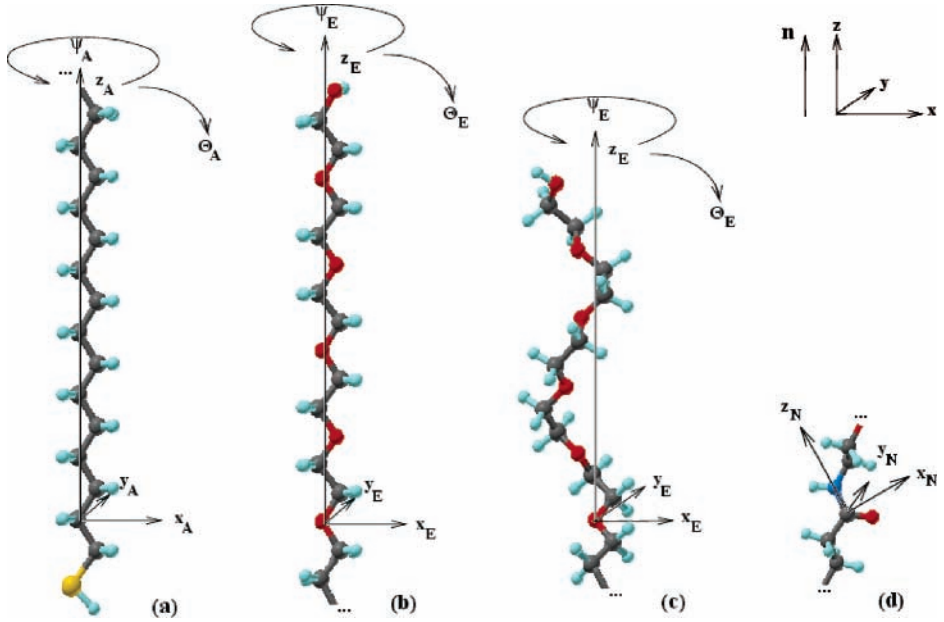

Figure 2. Definition of Euler angles and (x_A,y_A,z_A) axes for alkyl segment (a), (x_E,y_E,z_E) axes for OEG trans (b) and helix (c), and (x_N,y_N,z_N) for amide group (d). The axes are shown for the case when in the laboratory frame of reference *xyz*, all the angles are zero except $\theta_N = -30°$. In parts a and b of Figure 2, the x_Az_A- and x_Ez_E planes coincide with the CCC− and all-trans COC planes, respectively; for helical OEG conformation, axis x_E is directed along the bisector of the angle formed by the first COC group, axis z_E is the vector product of x_E and the bisector of the angle formed by the next COC group, and axis $y_E = z_E \times x_E$. For the amide moiety CONH, the z_N axis is parallel to the C−N bond, axis y_N is perpendicular to the O═C−N−H plane, and $x_N = y_N \times z_N$.

TABLE 1: Calculated Angles for Optimized Geometries of Molecules 1-t = $HS(CH_2)_{15}CONH-EG_4$ (trans), 2-t = $HS(CH_2)_{15}CONH-EG_6$ (trans), 2-h = $HS(CH_2)_{15}CONH-EG_6$ (helix), and 3-h = $HS(CH_2)_{11}CONH-EG_6$ (helix)[a]

	$\angle z_A/z_E$[b]	ψ_E^0	φ_E^0	θ_N^0	ψ_N^0	φ_N^0	τ(CCCN)	τ(CNCC)	τ(OCCO)
1-t	12°	−70°	101°	−43°	35°	113°	135°	−101°	180°
2-t	8°	−69°	104°	−45°	35°	122°	135°	−103°	180°
2-h	28°	87°	−69°	−41°	36°	103°	133°	−105°	72°
3-h	25°	83°	−69°	−40°	34°	101°	134°	−104°	72°

[a] Characteristic angles θ_E, ψ_E, φ_E, θ_N, ψ_N, and φ_N for $\theta_A = \psi_A = \varphi_A = 0$ and the following dihedral angles: angle of rotation with respect to the C−C bond, where the second carbon belongs to the amide group τ(CCCN), angle of rotation with respect to the N−C bond τ(CNCC), and angle of rotation with respect to the central C−C bond of OEG τ(OCCO). [b] $\angle z_A/z_E = \theta_E$ for $\theta_A = \psi_A = \varphi_A = 0$.

ties of SAMs consisting of complex molecular compounds (such as those which form OEG-terminated SAMs), there are two factors of crucial importance. These are the mutual orientations of the molecular building blocks and the orientation of the molecular skeleton with respect to the metal substrate surface. In our case, the molecular components are $HS(CH_2)_{11,15}$, undecanethiol and pentadecanethiol chains, CONH, an amide group, and $(CH_2CH_2O)_{4,6}H$, tetra(ethylene-glycol) only in the all-trans conformation and hexa(ethylene-glycol) in the all-trans and helical conformations.[2] The orientation of each of the components can be determined by the corresponding set of Euler angles. The first set, which specifies orientation of the alkyl CCC plane with respect to the substrate surface, is represented by θ_A, the angle of tilting of the z_A axis relative to the substrate normal **n**, the azimuthal angle φ_A, and ψ_A, the angle of rotation of the x_Az_A plane about the z_A axis.[11] Axes x_A, y_A, and z_A are introduced in an established manner;[12] see Figure 2a. Similarly, Euler angles θ_E, φ_E, and ψ_E give spatial orientation of the OEG part of the molecule. For the all-trans OEG chains, these angles determine the orientation of the COC plane, and their definition (in the $x_Ey_Ez_E$ frame of reference, see Figure 2b) is the same as that of θ_A, φ_A, and ψ_A with respect to the CCC plane. For helical OEGs, the x_E, y_E, and z_E axes can be defined as follows:[13] Axis x_E coincides with the bisector of the angle formed by one of the COC groups of the OEG chain (the first COC group in Figure 2c); axis z_E is the vector product of x_E and the bisector of the angle formed by the next COC group; axis y_E is determined by the vector product $z_E \times x_E$; see Figure 2c. Provided the orientation of the CCC plane is known, angles θ_E, φ_E, and ψ_E can be found from the transformation matrix from the $x_Ay_Az_A-$ to the $x_Ey_Ez_E$ system of coordinates.[11] Hence, one can find the orientation of the OEG portion (with respect to the substrate related frame of reference) for the given orientation of the alkyl portion of the molecule. Finally, the orientation of the amide moiety CONH is characterized here by x_N, y_N, and z_N; see Figure 2d. The direction of the z_N axis coincides with the C−N bond, axis y_N is perpendicular to the O═C−N−H plane, and $x_E = y_E \times z_E$. Then, the third set of Euler angles is given by θ_N, φ_N, and ψ_N, where θ_N is the tilting of the C−N bond with respect to the surface normal, φ_N is azimuthal angle, and ψ_N is the rotation of the O═C−N−H plane about the C−N bond.

Molecules **1-t**, **2-t**, **2-h**, and **3-h** in optimized geometries (found here with the help of BP86 method with a 6-31G* basis set) are shown in Figure 1. The angle $\angle z_A/z_E$ between alkyl (z_A) and OEG (z_E) axes within molecules **1**−**3** and the characteristic dihedral angles τ(CCCN), τ(CNCC), and τ(OCCO), which determine the structure of the molecules, are presented in Table 1. The angles of the OEG and O═C−N−H planes relative to the frame of reference coinciding with x_A, y_A, z_A for

$\theta_A = \psi_A = \varphi_A = 0$ (the CCC plane is lying in the *xz* plane in Figure 1) are also given. These angles θ_E^0 (equal to $\angle z_A/z_E$), ψ_E^0, φ_E^0, θ_N^0, ψ_N^0, and φ_N^0 describe the tilt and rotation of OEG and amide segments with respect to the alkyl plane.

For the helical and all-trans conformations of OEG, the angles between the z_A and z_E axes turned out to be quite different and close to 30° and 10°, respectively. Hence, for the all-trans conformation, angle $\angle z_A/z_E$ is considerably smaller, indicating that the OEG and alkyl axes are not too far from being parallel to each other despite the fact that they are linked via an amide bridge. This observation is consistent with the "stretched" model proposed for all-trans EG_3-terminated alkanethiols.[14,15] A comparison of the z_A/z_E angles found for the OEG-terminated alkanethiols with different lengths of the alkyl and OEG segments, exhibits certain trends in the dependence of $\angle z_A/z_E$ on molecular length. For example, the angle decreases with increasing length of the all-trans OEG chain, but it increases when the alkyl portion becomes longer; see Table 1.

We notice also that the value of ψ_E for the OEG helix depends on the choice of the origin of the $x_E y_E z_E$ system of coordinates. In our representation, the origin coincides with the oxygen of the first COC group. The difference in rotations of the OEG segment with respect to the surface normal **n** (the difference in φ_E values) for the all-trans and helical conformers is almost 180°. This indicates that the all-trans and helical OEG axes are tilted with respect to **n** almost in opposite directions. An immediate implication of this result is that the helical axis is tilted toward the N−H bond, while the all-trans OEG axis appears tilted toward the amide oxygen. The marked distinction between orientations of all-trans and helical OEG conformers is decisive in understanding the change of SAM thickness under the helical/all-trans transition; see subsection 3.3.

The conformation of the OEG portion is primarily determined by values of dihedral angles denoted below as τ(OCCO). Their values for the central OCCO group in molecules **1**−**3** are given in Table 1. The calculated values of τ(OCCO) are equal to 180° and 72° for the all-trans and helical conformations, respectively. Note that for poly(ethylene glycol), this angle is close to 70°.[13] Values of other dihedral angles τ(CCCN) and τ(CNCC), which determine the mutual orientation of alkyl and amide portions, are quite similar for both conformations of the OEG segment. This implies that for all four molecules under consideration, the orientation of the O═C−N−H plane is nearly the same, as evidenced by the data represented in Table 1. For example, the angles θ_N^0, ψ_N^0, and φ_N^0 display almost identical values for **1**−**3**. However, even a rather small difference in these angles for the all-trans and helix OEG can affect significantly the hydrogen bond length as discussed in subsection 4.4.

For the calculated optimized geometries, the amide group (CONH) in molecules **1**−**3** adopts the trans conformation, that is, the dihedral angle OCNH is close to 180°. As is known, this group also can exist in the cis conformation, for which τ(OCNH) is close to 10°. However, we found that the molecular geometries associated with the cis conformation of the CONH moiety give contradicting SAM characteristics. For example, the calculated thicknesses of corresponding SAMs turn out to be much smaller than those observed experimentally. Furthermore, we focus only at such optimized geometries, which place the amide oxygen out of the CCC (alkyl) plane. The reason is that there are a number of experimental facts (see below) which are not consistent with the inplane alignment of the C═O bond.

Obviously, there is no guarantee that the optimized geometries, which have been found here for isolated molecules, remain to be the most favorable ones when nearest- and next-nearest-neighbor interactions are included in the modeling. However, the demonstrated agreement between theoretical and experimental RA spectra certifies the reality of the suggested molecular structures and orientations and serves at least as a well-founded starting point for further studies of highly organized monolayer assemblies. Such studies are presently in progress at our laboratories.

3.2. Molecular Orientation within the SAM. To find the most likely orientation of the molecular constituents within the SAMs of **1**−**3**, we rely on the following experimental observations. It is known that amide I (C═O stretching) and amide A (N−H stretching) vibrations are absent in the RA spectra of OEG-containing SAMs.[16] In contrast, the amide II vibration (C−N−H inplane bending combined with C−N stretching) gives an intense peak at ∼1560 cm^{-1}. One can conclude therefore that the TDM of the amide II mode is aligned close to parallel to the surface normal **n**. At the same time, the TDM of the amide I mode, which is of a comparable magnitude with the TDM of amide II (as it follows from the comparison of amide I and amide II peaks in KBr transmission spectra[16]), appears to be close to perpendicular to **n**. Note that the TDMs of amides I and II are not parallel to their associated bonds C═O and C−N, respectively (see subsection 4.4). Taken together, these data put certain limitations on angles between C═O ($\gamma_{C=O}$) and C−N (θ_N) bonds and the SAM surface normal **n**.

Not less important are the experimental observations[2,16] suggesting that amide-containing SAMs are additionally stabilized by hydrogen bonding between amide groups, and that the strength of the developed hydrogen bond, and thereby the distance between H and O atoms in nearest-neighbor CONH groups may vary with OEG conformation. One should also take into account that the relative intensity of the symmetric and asymmetric peaks, which corresponds to CH-stretching vibrations of the alkyl chain, is strongly dependent on the orientation of the CCC plane.

All the above-mentioned requirements should be met in the modeling of the SAM structure. Our step-by-step procedure was as follows: (1) finding optimized geometry, (2) determining (from comparison of measured and calculated vibrational spectra) a range of values of θ_A and ψ_A, which is consistent with the intensities of symmetric and asymmetric peaks in the CH-stretching region, observed for alkanethiol self-assemblies,[12,17] (3) finding specific values of θ_A and ψ_A within that range, for which the angles $\gamma_{C=O}$ and γ_{N-H} are not too far from 90° and θ_N is not large, and (4) finding the values of the azimuthal angle φ_A that would provide the minimal distance between the oxygen atom from one of the CONH groups within the SAM and the hydrogen atom of the nearest-neighbor amide group, if the sulfur atoms form a hexagonal overlayer structure. Note that for the chosen value of φ_A, one also has to control the distance between the hydrogen atoms of the neighboring molecules to prevent them from being too close to each other.

As a result of the procedure outlined above we arrived at the values of θ_A, ψ_A, and φ_A which can be regarded as optimal; that is, they meet the best possible manner for all the requirements listed above. These values are summarized in Table 2. The orientation of the C═O bonds with respect to the substrate normal **n** (angle $\gamma_{C=O}$) and the corresponding values of θ_E, ψ_E, φ_E, θ_N, ψ_N, and φ_N angles are also given.

The tilt angle $\theta_A = 26$ fits well in the range of ∼26° to ∼40° which is known for related SAMs.[12,15,18,19] For example, in ref 12 it is evaluated to be ∼27° for the SAM of *n*-alkanethiols on a gold surface; the force-field modeling of metoxy tri(ethylene

TABLE 2: Characteristic Angles for Molecules 1−3

	θ_A	ψ_A	φ_A[a]	θ_E	ψ_E	φ_E[a]	θ_N	ψ_N	φ_N[a]	$\gamma_{C=O}$
1-t	26°	−62°	−80°	36°	−42°	−68°	−32°	−5°	3°	91°
2-t	26°	−65°	−82°	32°	−38°	−73°	−36°	−3°	4°	87°
2-h	26°	−62°	−77°	22°	25°	−151°	−27°	−4°	−3°	96°
3-h	26°	−58°	−79°	22°	16°	−143°	−26°	−8°	0°	97°

[a] For the hexagonal lattice, the change of the value of azimuthal angle by 60°·*n*, $n = 0, 1, ...$ does not affect the SAM structure.

glycol)-terminated alkanethiols in ref 15 gives $\theta_A \sim 37°$. In SAMs of alkylated 1-thiahexa(ethylene oxide) on gold, this parameter is found in ref 18 to satisfy $\theta_A = 32 \pm 2°$. Our modeling suggests that the value of θ_A should be restricted to $26 \pm 5°$; larger or smaller values lead to serious conflicts between the calculations and experimental data. Nearly the same constraints are found to be valid for the angles ψ_A and φ_A.

An important conclusion that follows from Table 2 is that the optimal angles for the alkanethiol chain are very similar for **1**−**3**. Hence the conformational properties and the length of the OEG tail only marginally influence the orientation of the alkyl segment. The predicted values of θ_A and ψ_A are consistent with the previous estimates of tilt/rotation of the alkyl chain in the SAM of *n*-alkanethiols on gold[17] and OEG-terminated SAM on gold.[3] For the obtained orientations, the calculated values of the angle $\gamma_{C=O}$ are close to 90°, an orientation that is consistent with a low intensity of the amide I peak in agreement with experimental data.[2,16] These arguments support the validity of our choice of the geometries of molecules **1**−**3** from a number of other possible realizations.

For the all-trans OEG terminus, the estimated value of $\theta_E \sim 35°$ agrees well with the results of force field modeling of EG_3-terminated alkanethiol monolayers self-assembled on Au.[15] Moreover, the validity of the present estimate is evaluated by calculating the SAM thickness (see below). The predicted value of $\theta_E \sim 22°$ for the helical conformer seems to be in contradiction with the prevailing belief in the field. Most references in the literature align the OEG helix axis within OEG-terminated SAMs parallel to the substrate normal **n**.[3,15,18,20] However, there is no direct experimental and/or theoretical proof of a strictly parallel orientation of the OEG helix to **n**. On the other hand, modeling of the RA spectra of **1**−**3** supports the estimated value of θ_E; see the next section.

The angles of the amide moiety in Table 2 demonstrate that the predicted values of θ_N (the angle between C−N bond and **n**) ensure the presence of a strong amide II peak in the RA spectra. Small (close to zero) values of angle of rotation of the amide segment with respect to the C−N bond (ψ_N) and of the azimuthal angle φ_N indicate that for optimal orientation of **1**−**3**, the CONH group is aligned almost parallel to the *xz* plane as in Figure 1.

3.3. OEG-SAM Thickness. For the obtained geometries and orientations of the molecular constituents **1**−**3**, we evaluate the thicknesses of the respective SAMs for a comparison with the experimental values. First we represent the molecular lengths of **1**−**3** (excluding the S−H bond) and the length of the alkyl and OEG segments. The results are shown in Table 3, where the molecular (or molecular segment) length is understood as the distance between the end atoms of the molecule (segment). These data allow one to compare the exactly calculated values of SAM thickness (fifth column of the table) with the approximate estimates equating the contributions of the alkyl and OEG portions to length of the segment × cosine of the tilt angle. For the angles given in Table 2, the contribution of amide group with the SAM thickness is equal to 3.7 ± 0.1 Å for **1**−**3** (the difference is small due to nearly the same orientation of the CONH group). This value, combined with the "thickness" of the alkyl and OEG portions, gives SAM thicknesses of 40.8 and 38.3 Å for **2-t** and **2-h**, respectively. This is very close to the exact values given in Table 3. The difference of ∼0.5 Å for the helical conformer is mainly due to the difference in tilt angles of z_E (equal to 22°, see Table 2) and of the vector connecting the first C and last H of the helical OEG segment (equal to 13°). Thus, these very simple considerations allow us to evaluate the contributions of all molecular segments into a proper SAM thickness.

TABLE 3: Comparison of Measured and Calculated SAM Thicknesses for Amide Group Containing OEG-Terminated Alkanethiols on Gold[a]

	alkyl chain length (Å)	OEG chain length (Å)	molecular length (Å)	calculated thickness (Å)	measured thickness[b] (Å)
1-t	19.5	13.8	36.6	33.9	33.3 ± 1.1
2-t	19.5	20.9	43.8	40.6	n.a.
2-h	19.5	16.4	38.6	38.9	39.8 ± 1.7
3-h	14.4	16.4	33.8	34.3	34.9 ± 1.1

[a] The calculated lengths of alkyl and OEG segments as well as of the whole molecules are also shown. [b] Experimental data from ref 2.

The thickness for SAMs consisting of molecules **1**−**3** is calculated for $\theta_A = 26°$ and the known S−Au distance (1.9 Å).[21] Within experimental errors, the estimated thicknesses agree very well with ellipsometric measurements.[2] Regardless of the substantial difference in length of the EG_6 portion for all-trans and helical conformations (the all-trans conformer is 4.5 Å longer), the thickness of **2-t** is only 1.7 Å larger than that of **2-h**. This can be explained with the help of the characteristic angles φ_A and φ_E shown in Table 2. For the optimal orientations of the alkyl chains, the difference in rotations of the OEG and alkyl segments with respect to the surface normal **n** (the difference between φ_E and φ_A values) for a helical conformer is more than 70°, while the values of φ_A and φ_E for an all-trans conformation are practically the same. The tilt of the z_E axis is substantially larger for the all-trans conformation than that for the helical OEG; see Table 2. It follows from these data that under the helical/all-trans transition, the effective tilt (i.e., the angle between the normal and straight lines connecting the sulfur atom and hydrogen atom of the OH end group) increases from 17° to 28°. Hence, the larger length is compensated by the larger effective tilt.

4. Modeling of IR Response

It is well-known in RA spectroscopy of thin layers on metallic supports that it is only the vibrational modes having TDMs aligned perpendicular to the metal substrate that appear in the spectra. The model SAM spectra (solid lines in Figure 3) are calculated according to eq 3. We found it sufficient to use only two values of the parameter σ. Namely, $\sigma = 6$ cm^{-1}, for the peaks that are due to the OEG helix vibrations and $\sigma = 12$ cm^{-1} for the OEG all-trans and amide peaks. The value of I_0 is the same in all calculations, and as already mentioned, the frequencies of amide II and amide III vibrations are multiplied by scaling factor 1.037. No other fitting was used to model spectra **1**−**3** which are shown for the values of θ_A and ψ_A given in Table 2.

4.1. All-Trans OEG Molecules 1-t, 2-t. IR RA spectra of the corresponding all-trans SAMs have been reported earlier.[1,2] Here they are compared with the model RA spectra of molecules **1-t** and **2-t** in Figure 3a (the spectra are off-set for clarity). The most distinctive peaks and their assignments are also represented

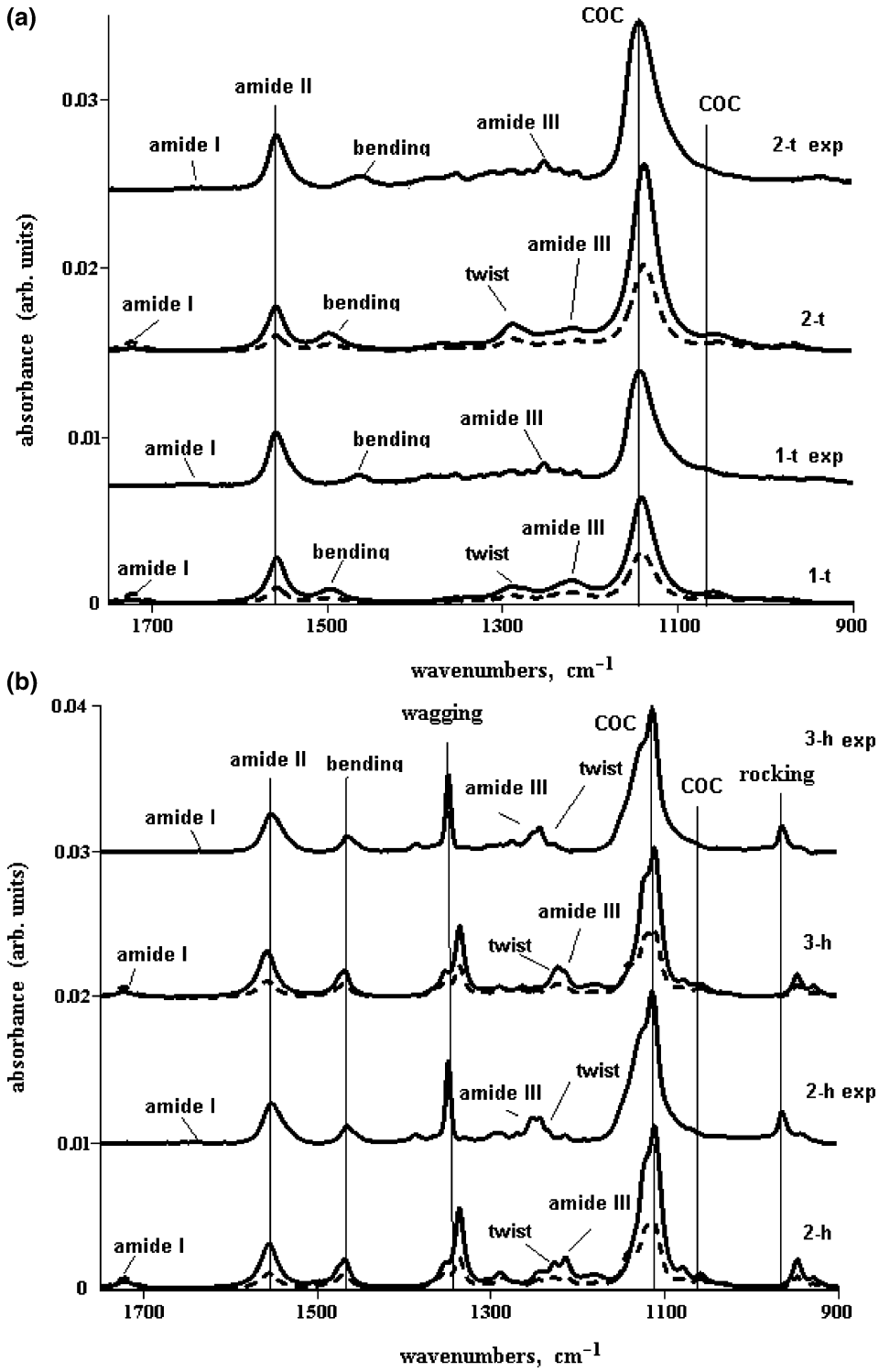

Figure 3. (a) Comparison of measured and calculated spectra of **1-t** and **2-t** in the fingerprint and amide regions. hwhm = 12 cm^{-1} for all peaks. The scaling factor for amide II and amide III peaks equals 1.037. (b) Comparison of measured and calculated spectra of **2-h** and **3-h** in the fingerprint and amide regions. hwhm = 6 cm^{-1} for the fingerprint region and 12 cm^{-1} for the amide peaks. The scaling factor for amide II and amide III peaks equals 1.037.

in Table 4. The calculated frequencies in the fingerprint region are very close to those observed experimentally, and this is particularly evident for the most intense peak in this region that is attributed to the asymmetric skeletal C−O−C stretching mode; see Figure 3a. This peak is observed at 1144 cm^{-1} and is reproduced by our calculations as a superposition of several strong C−O−C stretching modes forming a peak at 1140 cm^{-1}. Our calculations also assign a small, partly resolved feature on the low-frequency side of this peak to the same C−O−C stretching vibrations. The other modes do not form pronounced peaks in either the calculated or the measured spectra, except for a few rather weak peaks that are due to the twisting amide III and bending CH_2 vibrations. The striking similarity of the modeled and measured spectra supports the statement that the OEG segments of molecules **1-t** and **2-t** adopt the all-trans conformation. The same conclusion has been drawn before by comparing the measured spectra of **1-t** and **2-t**, with the spectrum of an EG_3 SAM on silver.[14−16]

TABLE 4: Calculated and Measured Vibrational Frequencies (in cm^{-1}) and Their Assignments for the All-Trans OEG-Terminated Amide-Linked Alkanethiols[a]

1-t calculated	**1-t** observed[b]	**2-t** calculated	**2-t** observed[b]	assignment
1057	~1060	1058	~1060	asymmetric C−O−C stretching
1141	1144	1140	1144	asymmetric C−O−C stretching
1221, 1273	1253	1221, 1273	1253	amide III
1498	~1465	1498	~1465	CH_2 bending
1557	1559	1559	1559	amide II

[a] Frequencies of amide II and III vibrations are scaled by 1.037. [b] Experimental data from ref 2.

The model spectra of **1-t** and **2-t** seem almost identical except for the expected difference in absolute peak intensities. The same observation is true for the experimental RA spectra. We found also that a variation of the angle θ_A within 10−15° and ψ_A from 0 to 360° resulted in changes in the relative intensity of the amide I, amide II, and C−O−C stretching peaks, whereas the other peaks remained essentially unaffected. This statement is illustrated by dashed lines in Figure 3a which model the spectra of randomly oriented molecules **1-t** and **2-t**, defined as in eq 3. For the values of θ_A and ψ_A given in Table 2, the calculated intensity ratio for the two main peaks in this region (C−O−C stretching near 1140 cm^{-1} and amide II near 1550 cm^{-1}) is almost the same as those in the measured spectra; see Figure 3a.

While many details in measured and calculated RA spectra are similar, there are some minor omissions in the reproducibility. It is worthwhile to mention that the asymmetry of the main peak is clearly observed experimentally but not in the calculated spectra. The reason is that the main peak emanates from a number of coupled modes whose relative intensity and position are not reproduced exactly by the ab initio methods. Also, a small fraction of conformers other than all-trans might coexist in real SAMs.

4.2. Helical OEG Molecules 2-h, 3-h. At room temperature the EG_6 moiety is known to adopt the helical conformation. We performed modeling of RA spectra of OEG-terminated alkanethiols with helical OEG segments **2-h** and **3-h** to investigate the differences in RA spectra accompanying the all-trans/helical transition. To trace the role of the alkyl segment, we calculated the vibrational spectra for two molecules with the same OEG portion but different alkanethiol chains, $HS(CH_2)_{11}$ and $HS(CH_2)_{15}$. Model RA spectra of molecules **2-h** and **3-h** are compared with experimental RA spectra [1,2] in Figure 3b. Since the OEG portions of molecules **2-h** and **3-h** are the same and the mutual orientation of alkyl and OEG segments is rather close for these two molecules (see Table 2), a comparison of their vibrational spectra reveals the influence of the alkyl segment. Figure 3b shows that the alkyl modes contribute to the region with rocking, twisting, and amide III peaks, but the intensities are rather weak. This is the consequence of the known fact that it is only the OEG portion that contributes to the apparent spectrum in this frequency region.

It is seen that the simulated spectra of **2-h** and **3-h** reproduce quite well the relative positions and intensities of all significant features of the experimental RA spectra. The assignment of fundamental OEG modes completely agrees with previous findings.[1−3,13−16,18,20] It is also seen from Table 5 that the unscaled frequencies deviate from the measured values by only ~2%. The weak feature observed at the low-frequency side of the main peak is attributed to asymmetric COC stretching combined with OEG CH_2-rocking vibrations. A peak near 1200−1250 cm^{-1} in the measured and calculated spectra contains a contribution from several CH_2-twisting and amide III modes.

The shape of the measured spectra with a pronounced asymmetry of the dominating peak is reproduced remarkably well by our calculations. The high-frequency shoulder is often attributed to the presence of nonhelical conformational states in the OEG SAMs, since amorphous and all-trans OEGs absorb in the region 1125−1150 cm^{-1}.[14−16,18,20] In the model spectra, the shoulder of the main peak appears because of a substantial tilt of the z_E axis which exposes the modes with large TDMs in the *x*,*y* directions. Hence, an alternative and plausible explanation of the peak asymmetry may be the multimode structure of the C−O−C stretching peak. The relative contribution of modes with different TDM orientations is illustrated in Figure 3b by dashed lines modeling the spectra of randomly oriented **2-h** and **3-h** molecules. It is seen that there exist several strong C−O−C stretching modes that have comparable values of $(\mu_{x,y}^{(i)})^2$ and $(\mu_z^{(i)})^2$. Similar arguments in favor of nonparallel orientation of the helix axis with respect to the surface normal can be inferred from analysis of spectroscopic data obtained for the CH_2-stretching region.[8]

4.3. Distinctions between RA Spectra of All-Trans and Helical OEG SAMs. The initial and final states of the helical to all-trans transition are represented by the RA spectra in Figure 3. A significant decrease of the peak intensities of the rocking, wagging, and bending modes is observed when passing from helical to all-trans OEG-terminated SAMs. In addition, a very pronounced feature of the RA spectra in the fingerprint region is the blue shift of the main OEG peak from 1114 cm^{-1} for helical to 1144 cm^{-1} for all-trans.[1,2] Our calculations place the main peak at 1111 and 1140 cm^{-1} for **2-h** and **2-t**, respectively, a shift of 29 cm^{-1} that correlates with the experimentally measured difference of 30 cm^{-1}.[1] Such an excellent agreement between experimental and theoretical values strongly supports our earlier interpretation of spectral changes observed under the reported phase transition.[1]

4.4. Amide Absorption Peaks. As already mentioned, the amide II vibration produces an intense peak in the RA spectra

TABLE 5: Calculated and Measured Vibrational Frequencies (in cm^{-1}) and Their Assignments for the Helical OEG-Terminated Amide-linked Alkanethiols[a]

2-h calculated	**2-h** observed[b]	**3-h** calculated	**3-h** observed[b]	assignment
947	964	947	964	CH_2 rocking and asym. C−O−C stretching
1079	~1050	1078	~1050	CH_2 rocking and asym. C−O−C stretching
1111	1114	1111	1114	asym. C−O−C stretching
1214, 1227, 1290	1243	1214, 1224, 1290	1243	CH_2 twisting
1223, 1233	1252	1223, 1239	1252	amide III
1336	1349	1336	1349	CH_2 wagging
1467	1464	1467	1464	CH_2 bending
1555	1553	1558	1552	amide II

[a] Frequencies of amide II and amide III vibrations are scaled by 1.037. [b] Experimental data from ref 2.

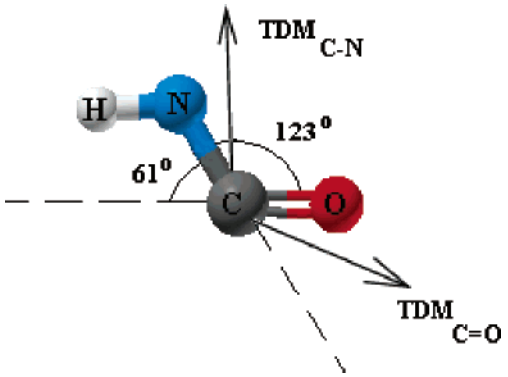

Figure 4. Structure of amide group (CONH). Arrows indicate the directions of TDMs.

of SAMs containing amide linkages (see ref 16 and references therein). In contrast, the amide A and amide I vibrations are practically invisible. Furthermore, from a comparison of the amide II peak intensity in SAM RA spectra of compounds **1-t** and **2-t** with those in the corresponding KBr transmission spectra,[16] it was concluded that the corresponding TDM components in the *x*,*y* directions are very weak for a highly oriented assembly. Thus, it is instructive to see how our optimal molecular orientation fully agrees with these experimental observations.

Our calculations suggest that the amide link is a rigid entity and that its geometry is practically the same in all our compounds. It was also found that the length and conformation of the molecular chains linked by the amide group have little effect on the mutual orientation of the amide TDMs. Moreover, the calculations show that TDM_{C-N} and $TDM_{C=O}$ are not parallel to their respective bonds, that is, the $\angle TDM_{C-N}/C-N \sim 20°$ and $\angle TDM_{C=O}/C=O \sim 20°$ and they are not parallel to the O=C−N−H plane. As a consequence, the angle $\angle TDM_{C-N}/TDM_{C=O}$ turns out to be near 120°, that is, very close to ∠OCN; see Figure 4. These data can be explained by the fact that the amide I (or II) mode involves more complex motion than just C=O (or C−N) stretching vibrations. For the molecular geometries and orientations of **1**−**3** obtained in our study, we found that the angles between TDM direction and substrate normal **n** is ∼10° ($\theta_N \sim 30°$) for amide II and ∼110° ($\gamma_{C=O} \sim 90°$) for amide I. Hence, the orientation of TDM_{C-N} leads to nearly maximal intensity of the amide II peak, which agrees well with experimental results, and suggests also a preferential orientation of $TDM_{C=O}$ parallel to the surface. Notice that a better parallel alignment of $TDM_{C=O}$ along the substrate surface would result in a less favorable alignment of TDM_{C-N} with **n** and a substantial drop in amide II intensity.

4.5. Lateral Hydrogen Bonding. As it was first shown in ref 2, the observed amide II peak shifts by 6 cm^{-1} to higher frequencies during the helix/all-trans conformational transition in SAMs of $HS(CH_2)_{15}CONH-EG_6$, that is, the transition from **2-h** to **2-t**. The shift from 1553 cm^{-1} in **2-h** to 1559 cm^{-1} in **2-t** was attributed to a strengthening of NH···O=C hydrogen bonding in the all-trans conformation. To validate that conclusion, we calculated the hydrogen bond lengths, which can be expected for the SAM consisting of **1**−**3**. In the calculations, we assume that the molecules are arranged in a hexagonal overlayer structure ($\sqrt{3} \times \sqrt{3}$)R30° relative to the Au(111) substrate[19,22] with one molecule per unit cell. The postulated overlayer structure corresponds to a sulfur−sulfur spacing of ∼5 Å. Models with more than one molecule per unit cell are ruled out due to packing reasons.[15] Of course, such an assumption leaves out of consideration intriguing but poorly understood issues of the adsorption behavior and effects associated with adsorbate−substrate and intermolecular interactions within SAMs.[19] In the absence of more established adsorption data and because of the existing controversy regarding theoretical predictions of the sulfur adsorption sites,[15,19,23] the hexagonal structure seems to be most plausible for a zero-order evaluation of lateral hydrogen bonding phenomena as well as molecular orientation.

For the molecular orientations represented in Table 2, we obtain the following distances between the amide hydrogen and the oxygen of the nearest-neighbor CONH group, 2.2 Å for **2-t** and 2.6 Å for **2-h**. Clearly, the predicted hydrogen bond length decreases when passing from the helical to the all-trans conformation. The same tendency was revealed for the SAMs consisting of **1-t** and **3-h** molecules, where this distance equals 2.3 Å for **1-t** and 2.6 Å for **3-h**, respectively. These estimates suggest that the amide group possesses a more favorable orientation for hydrogen bond formation in SAMs with the OEG portion in the all-trans conformation. This observation is consistent with recent experimental observations by Valiokas et al.[2] who suggested that favorable lateral hydrogen bonding contributed to the formation of a stable all-trans structure of EG_6 SAMs at elevated temperatures, >60 °C. The calculated values of (scaled) frequencies of the amide II peak in **2-h** and **2-t** are 1555 and 1559 cm^{-1}, respectively. This means that the calculated position of the amide II peak is 4 cm^{-1} blue shifted in the **2-t** compound. Changes in the OEG and alkyl chain lengths weakly influence the position of the peak; we obtained, respectively, 1557 and 1558 cm^{-1} for **1-t** and **3-h**. Thus, the observed blue shift cannot be attributed to a conformational change in the OEG segment but rather to a more favorable (from the point of view of hydrogen bond formation) alignment of nearby amide links in the corresponding SAMs.

5. Conclusion

In this study we have examined by means of ab initio modeling the structural properties of all-trans and helical OEG-terminated and amide-linked alkanethiols on gold. The work is motivated and justified by the manifestations of these conformational states in recent studies of temperature-driven phase transitions of OEG-SAMs. Optimized molecular geometries and relative orientation within the self-assemblies of compounds **1**−**3** on a Au(111) substrate have been deduced in a quantitative manner from comparison of ab initio (DFT) modeled and observed RA spectra. It is shown that a good consistency with known experimental data can be obtained if the alkyl CCC plane is tilted by $\theta_A = 26°$ and rotated by ψ_A (−65° to −58°) depending on the choice of molecules **1**−**3**. These angles demonstrate an impressive agreement between experimental and modeled spectra in the fingerprint and amide regions. Such an agreement favors the molecular orientation parameters (tilts and rotations) proposed in our study and allows us to predict the precise orientation of the alkyl and OEG portions within the SAM. Distinctions between experimental RA spectra of all-trans and helical OEG SAMs appear in the same manner in modeled spectra, which gives additional proof for our earlier interpretation of spectral changes observed under the all-trans to helical phase transition.[1]

For the predicted values of the azimuthal angles ($\varphi_A = -82°$ to −77°), we found that the spacing between the nearest-neighbor amide groups in the all-trans and helical OEGs (organized in a hexagonal overlayer structure) is consistent with the experimentally observed variation in lateral hydrogen bonding between neighboring C=O and N−H groups. More-

over, the calculated hydrogen bond lengths tend to decrease under the helical to all-trans transition demonstrating a more favorable molecular orientation in the all-trans OEG SAMs. We have verified this statement by modeling an assembly of OEG-terminated amide-linked alkanethiols by means of molecular mechanics, starting from the proposed optimized geometries and orientation parameters. The AMBER force field modeling of **2-t** and **2-h** 16 × 16 clusters confirms the tendency of strengthening of the hydrogen bonding in all-trans OEG SAMs. A molecular mechanics study on the role of intermolecular and molecule−substrate interactions within OEG SAMs will be published separately.

Acknowledgment. The authors thank the Swedish Research Council (VR) and the Swedish Foundation for Strategic Research (SSF), through the Biomimetic Materials Science program, for financial support.

References and Notes

(1) Valiokas, R.; Svedhem, S.; Svensson, S. C. T.; Liedberg, B. *Langmuir* **1999**, *15*, 3390.

(2) Valiokas, R.; Östblom, M.; Svedhem, S.; Svensson, S. C. T.; Liedberg, B. *J. Phys. Chem. B* **2001**, *105*, 5459.

(3) Harder, P.; Grunze, M.; Dahint, R.; Whitesides, G. M.; Laibinis, P. E. *J. Phys. Chem. B* **1998**, *102*, 426.

(4) Gejji, S. P.; Tegenfeldt, J.; Lindgren, J. *Chem. Phys. Lett.* **1994**, *226*, 427.

(5) Jaffee, R. L.; Smith, G. D.; Yoon, D. Y. *J. Phys. Chem.* **1993**, *97*, 12745.

(6) Wang, R. L. C.; Kreuzer, H. J.; Grunze, M. *Phys. Chem. Chem. Phys.* **2000**, *2*, 3613.

(7) Buck, M. *Phys. Chem. Chem. Phys.* **2003**, *5*, 18.

(8) Malysheva, L.; Klymenko, Yu.; Onipko, A.; Valiokas, R.; Liedberg, B. *Chem. Phys. Lett*. **2003**, *37*, 451.

(9) Malysheva, L.; Onipko, A.; Valiokas, R.; Liedberg, B. *Appl. Surf. Sci.* **2005**, *246*, 372.

(10) Valiokas, R.; Östblom, M.; Svedhem, S.; Svensson, S. C. T.; Liedberg, B. *J. Phys. Chem. B* **2002**, *106*, 10401.

(11) Wilson, E. B., Jr.; Decius, J. C.; Cross, P. C. *Molecular Vibrations*; McGraw-Hill: New York, 1955.

(12) Parikh, A. N.; Allara, D. L. *J. Chem. Phys*. **1992**, *96*, 927.

(13) Miyazawa, T.; Fukushima, K.; Ideguchi, Y. *J. Chem. Phys.* **1962**, *37*, 2764.

(14) Harder, P.; Grunze, M.; Dahint, R.; Whitesides, G. M.; Laibinis, P. E. *J. Phys. Chem. B* **1998**, *102*, 426.

(15) Pertsin, A. J.; Grunze, M.; Garbuzova, I. A. *J. Phys. Chem. B* **1997**, *102*, 4918.

(16) Valiokas, R.; Östblom, M.; Svedhem, S.; Svensson, S. C. T.; Liedberg, B. *J. Phys. Chem. B* **2000**, *104*, 7565.

(17) Laibinis, P. E.; Whitesides, G. M.; Allara, D. L.; Tao, Y.-T.; Parikh A. N.; Nuzzo, R. G. *J. Am. Chem. Soc*. **1991**, *113*, 7152.

(18) Vanderah, D. J.; Meuse, C. W.; Silin, V.; Plant, A. L. *Langmuir* **1998**, *14*, 6916.

(19) Schreiber, F. *Prog. Surf. Sci*. **2000**, *65*, 151.

(20) Vanderah, D. J.; Pham, C. P.; Springer, S. K.; Silin, V.; Meuse, C. W. *Langmuir* **2000**, *16*, 6527.

(21) Sellers, H.; Ulman, A.; Shnidman, Y.; Eilers, J. E. *J. Am. Chem Soc.* **1993**, *115*, 9389.

(22) Ulman, A. *Chem. Rev.* **1996**, *96*, 1533.

(23) Fisher, D.; Curioni, A.; Andreoni, W. *Langmuir* **2003**, *19*, 3567.